Spatial and Temporal Analysis of Rain Gauge Data and TRMM Rainfall Retrievals in Hong Kong

Wing Fung James WONG[1], Long Sang CHIU[2*]

[1]Department of Geography and Resources Management, The Chinese University of Hong Kong, Hong Kong SAR, PRC
E-mail: james2068@yahoo.com
[2]Institute of Space and Earth Information Science, The Chinese University of Hong Kong, Hong Kong SAR, PRC
E-mail: longchiu@cuhk.edu.hk

Abstract
Tropical Rainfall Measuring Mission (TRMM) rainfall products ((precipitation radar (PR) 2A25 and 3B42 or TMPA)) and hourly rainfall data in Hong Kong from January 1, 1998 to December 31, 2007 were used to examine the spatial and temporal rainfall structure and their relation in Hong Kong. The hourly gauge data show a spatial decorrelation distance of about 28 km. There are large inter-annual variability of satellite and gauge rain rate distributions and their relations; however, there are consistent differences in the rain rate distribution between gauge and TRMM products. Analyses of rainy pixels between gauge and PR show small biases, decreasing root mean square error, mean absolute error for increasing grid sizes. The correlation coefficients between TRMM PR and hourly gauges data improved from 0.16, 0.34, to 0.52 for 0.1, 0.2 and 0.4 degree gridded rain rates, in that order. For TMPA 3-hourly 0.5 degree rainfall rates, the correlation coefficient is 0.35, with large inter-annual variations.
Keywords
TRMM, TMPA, spatial-temporal analysis, rainfall

I. INTRODUCTION

Accurate estimation of precipitation is vital for assessing and managing water resources for human consumption and for our living environment. Each year, floods and droughts cause loss of human lives and billions dollars of damages. However, reliable measurements of precipitation from ground are limited to very few areas of the worlds. The majority of the continental land surfaces and most of the oceans are not well monitored. The high temporal and spatial variability of rainfall makes space/time rainfall difficult to measure.

Measurement of precipitation from space complements ground-based measurements to provide a more complete picture of rain system structure. Satellite remote sensing techniques have been developed for decades. The Tropical Rainfall Measurement Mission (TRMM) is the first coordinated international effort to provide reliable rainfall measurement from space. The TRMM measurements provide the impetus for rain algorithm development and improvement.

There are a number of comparisons between TRMM rainfall products with other rainfall measurement. These studies have concentrated on the rain retrieval uncertainty issue at large spatial and temporal scales (daily, monthly and yearly) using error statistics (Ebert E, et al., 2007; Huffman G J, et al., 2007, 1995). Comparisons at the sub-daily scale are rare, due to the lack of validation data. These statistics are useful in assessing the use of satellite data for large-scale monitoring, water resource management, and hazard warning.

The purpose of this study is to show the potential utility of satellite rain observations in regional rain rate estimates. As a coastal city in the subtropics, Hong Kong is affected by both monsoon rainfall and typhoons. The spatial/temporal rainfall structure in Hong Kong is first examined. An assessment of the rainfall rate estimates by the TRMM Precipitation Radar (PR) and the TRMM Multi-sensor Precipitation Analysis (TMPA) is made by quantifying the associated uncertainty at different spatial and temporal scales. Geospatial tools will be used to estimate areal precipitation using information provided by the satellite borne PR and TMPA. Satellite and gauge network provide different and complementing rainfall information. Satellite data provide instantaneous pixel area-averaged rainfall with relatively poor time sampling (once or twice a day on average). The merge satellite/gauge TMPA is a three-hour average 0.25 degree rain rate. The gauges provide point measurement with good temporal resolution.

Section II provides a description of the data and the procedure for analysis. The results are presented in Section III. Section IV contains the summary and discussion about future work.

II. DATA AND METHOD

Two TRMM rainfall products are examined - TRMM 2A25 (PR Instantaneous Rainfall Rate and profile) and Version 6 3B42 3-hourly mean rainfall rate (or TRMM Multi-satellite Precipitation Analysis, TMPA).

TRMM PR 2A25 uses a hybrid of the Hitschfeld-Bordan method and the surface reference method to estimate the

*Department of Geography and Geoinformation Science, George Mason University, Fairfax VA USA

1082-4006/08/14(02)-105$5.00

vertical profile of attenuation-corrected effective radar reflectivity factor (Ze). The vertical rain profile is then calculated from the estimated Ze profile by using an appropriate Ze-R relationship. The 2A25 pixels represent snapshots (instantaneous) of rain rate maps with a horizontal resolution of 4.3 km at nadir and about 5 km at the scan edge (Gebremichael M, et al., 2008). Due to the curvature of the Earth's surface, the PR cannot measure precipitation rates very close to the ground at scan edge. There are also uncertainties at nadir due to the large surface reflection. Therefore, surface rain rates are inferred from the reflectivity profile above the surface (Bowman Kenneth P, 2005).

The TMPA or V6 3B42 is a 3-hourly, 0.25° product (TMPA; Huffman G J, et al., 1995). First, all available TRMM Combined Instrument (TCI)-calibrated microwave estimates, from TRMM Microwave Imager (TMI), Special Sensor Microwave Imager (SSM/I), Advanced Microwave Scanning Radiometer (AMSR), and Advanced Microwave Sounding Unit (AMSU), are put into the appropriate space–time bins. Microwave-calibrated IR rain estimates fill the remaining bins. These instantaneous estimates are summed over a calendar month to create a monthly multi-satellite (MS) product. The MS and gauge analysis (from Global Precipitation Climatology Center (GPCC) or Climate Analysis and Monitoring System (CAMS)) are merged optimally to create a post-real-time satellite-gauge (SG) monthly 0.25° product. The final TMPA is computed by scaling the intermediate SG by the ratio of monthly MS to SG [the scale factor being limited to a range (0.2, 2)]. The gauge analyses (GPCC or CAMS) employed are presented on a 2.5° or 1° grid, so that the fine scale spatial and temporal information in the 0.25° 3B42 and 3B43 data are attributed to satellite inputs (Chokngamwong R, and Chiu, 2008).

These TRMM data are downloaded from the NASA/GSFC/ Data and Information Service Center (DISC). The file size of the PR data is substantial (12GB/day) and hence only PR swath data within the grid box 21.1°–21.6°N, 113.9°–114.5° E are considered in this study. Not all TRMM overpass Hong Kong covered all Hong Kong territory. Partial orbit coverage will limit the data for comparison with ground rain gauges data. Even for coincident subsets, the existence of rain was rarely found. Only coincident subsets of PR data with rain and full coverage of study area from TRMM are considered. There are between 15 to 31 coincident rainy orbits available for analysis each year. A total 225 TRMM orbits over the ten year period are coincident with rain gauges. These include 31, 27, 17, 24, 19, 18, 15, 26, 24 and 24 orbits for 1998, 1998, ..., and 2007.

The hourly rainfall data of Hong Kong from 1998 to 2007 were available from Hong Kong Observatory. Figure 1 shows the location of the Automated Weather Station (AWS) gauges. Table 1 lists the coordinates and altitude of the AWS gauge location.

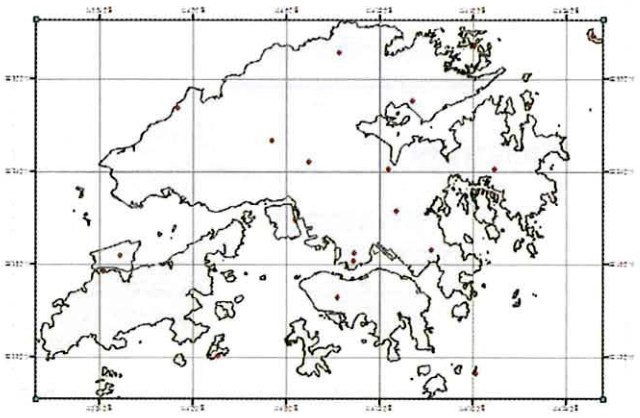

Figure 1. Map of Hong Kong, the study area and the location of the AWS rain gauges

Table 1. Locations and characteristics of weather stations as of 31 December 2006 (From: Hong Kong Observatory)

Station number	Code	Station	Position		Instrument elevation (in metres above MSL)		
			Latitude (° ′ ″)	Longitude (° ′ ″)	Anemo Meter	Baro Meter	Ground
45007	HKA	Chek LAP KOK airport(AMOS)	22 18 33.73	113 55 19.43	–	7.6	6
45004	CCH	Cheung Chau	22 12 04.04	114 01 36.00	98.5	79.8	71.9
	CPH	Ching PAK house, Tsing Yi	22 20 59.51	114 06 24.43	136	–	125
45005	HKO	Hong Kong observatory	22 18 12.82	114 10 18.75	73.8	62.2	31.8
45033	KAT	KATO(Agriculture and fisheries office)	22 32 10.90	114 18 07.00	–	–	9.6
45004	KP	King's park	22 18 47.00	114 10 14.00	89.63	66	64.8
45035	LFS	Lau Fau Shan(Police station)	22 28 14.29	113 58 52.42	49.7	35.5	34
45031	EPC	Ping Chau(Police post)	22 32 53.50	114 25 32.70	39.3	–	29.3
45042	SLW	Sha Lo Wan	22 17 33.08	113 54 16.32	70.9	–	58.4
45039	SHA	Sha Tin(Racecourse)	22 24 17.14	114 12 23.76	16	7.99	7
	SEK	Shek Kong	22 26 01.67	114 05 06.47	26.42	25.31	16.01
45032	TKL	Ta KWU ling(Pig breeding centre)	22 31 50.15	114 09 13.34	27.6	13.5	12
45034	PLC	Tai Mei Tuk(Police training centre)	22 28 36.30	114 14 06.30	70.8	–	–
	TMS	Tai Mo Shan	22 24 39.60	114 07 29.45	968.57	940.3	944.61
45047	TPO	Tai PO(Island house)	22 26 45.15	114 10 43.90	–	16.1	14.6
45036	TAP	TAP Mun(Police post)	22 28 22.40	114 21 29.40	37.1	–	–
45010	TC	Tate's cairn	22 21 34.00	114 12 55.00	588	–	575
	TYVV	Tsak Yue Wu	22 24 10.59	114 19 23.55	22.7	–	5.03
45041	JKB	Tseung Kwano(Haven of hope hospital)	22 19 03.00	114 15 15.00	51.6	–	32.3
45045	WGL	Waglan island(Station, VTS)	22 11 01.00	114 18 02.00	82.1	60.4	55.8

The hourly rainfall data were obtained from the network consisting of 20 gauges. These AWS gauges were chosen in order to maximize the coverage. As the AWSs are not evenly distributed statistical methods were used to estimate the data in between stations. Missing data existed in the observation records. Rain gauge data have been checked to ensure the quality of the records. Quality control includes verifying gauge coordinates against GIS maps and removal of missing and ambiguous records. To fill the missing data gaps, it is assumed that stations data can be interpolated spatially using an inversed distance relationship.

For comparison with TMPA, 3-hour mean rainfall rate from hourly rain gauge data was calculated. As the TRMM products are using UTC (Z) time, rain gauges data are shifted by 8 hours (time difference). For example, when 3B42 data is 00Z, the local time is 08 Hong Kong.

The TRMM Science Data and Information Service Center (TSDIS) developed the TSDIS OrbitViewer for visualizing and generating TRMM orbit and data information in ASCII format which can be used for analysis. Figure 2 shows the near surface rain data on September 2, 2003, using TRMM OrbitViewer when TRMM pass overhead Hong Kong at 23:00 local time. The data can be further zoomed to display the PR data over Hong Kong. The colour dots show the nadir position of each PR pixel position and the colour shows the rain intensity(Figure 3).

Figure 4 shows the PR pixel rain rates with locations data converted to ArcView shapefiles. ArcView is a geographic information system (GIS) software for visualizing, managing, creating, and analyzing geographic data. ESRI ArcGIS Geostatistical Analyst (GA) is an extension of ArcGIS 9.2 that helps to analyzing spatial problems by using various interpolation methods.

The evaluation of instantaneous products was based on

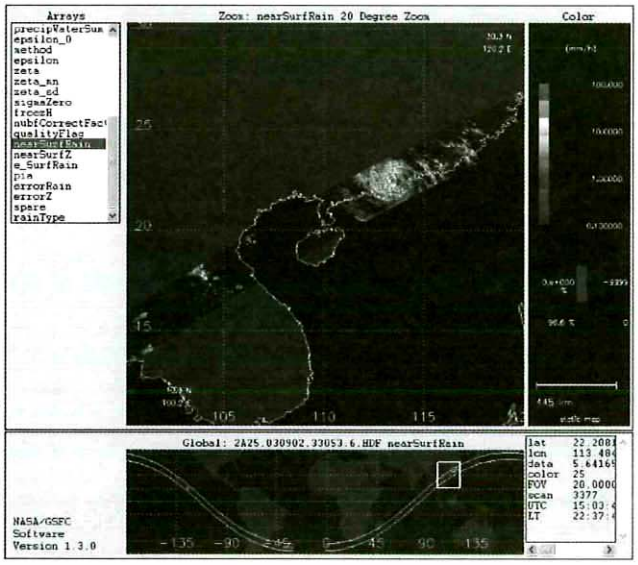

Figure 2. TSDIS Orbit Viewer display of near Surface Rain on 3 September 2003 at approximately 2300 local time

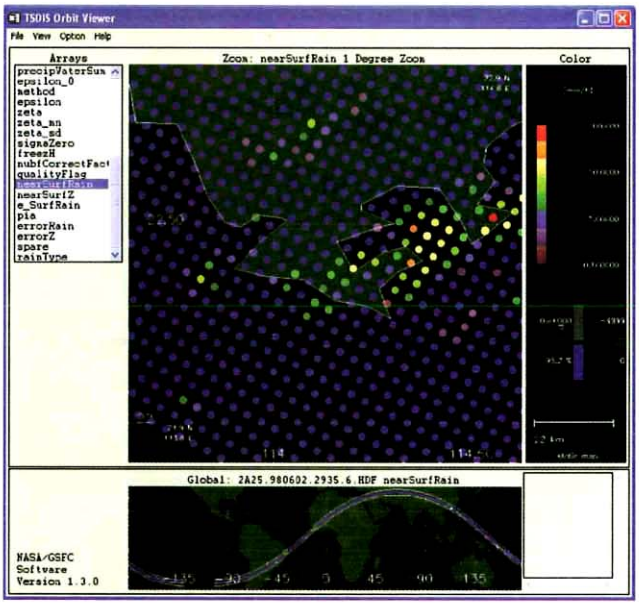

Figure 3. TSDIS Orbit Viewer image of TRMM PR overpass Hong Kong on 1998-06-02

comparing the distribution of rain rates as derived from the PR estimates over the gauges. However, due to the spatial variability of gauges, the distribution of the gauge rain rates does not necessarily represent the true distribution of rainfall rate at the scale of a radar pixel.

Spatial interpolation is needed for the gauge records since there are missing station data in addition to the gaps. The Inverse Distance Weighting interpolation (IDW) method is applied to both gauge and satellite pixel data. IDW interpolation determines cell values using a linearly weighted combination of a set of sample points. The weight is a function of inverse distance and closer points are more influence than distant points. The surface being interpolated should be that of a location dependent variable. IDW assigns weights to neighboring observed values based on distance to the interpolation location and the interpolated value is the weighted average of the observations. If only the next neighbor is considered (i.e. n=1), IDW collapses to the Thiessen polygon. Figure 5 shows the IDW for one neighbour.

Figure 6 shows the layer with IDW gauge data converted to a raster layer with 0.1 degree cell size. The grid cell value is equal to averaged of all interpolated rain gauges values inside the cell. For TRMM orbits that passed over Hong Kong, the locations of each PR footprint were mapped onto Hong Kong map (Figure 3).

On average there are 3 PR pixels within each 0.1 degree cell. The PR rain map is generated by Inverse Distance Weighted Method (IDWM) with 3 neighbors (Figure 7). Both Figure 5 and 7 shows three strips of high rain areas oriented NW-SE and thus gives the first indication that the PR provide qualitative rain information as the gauge. The PR rain map is converted into raster map with the same extent as AWS raster

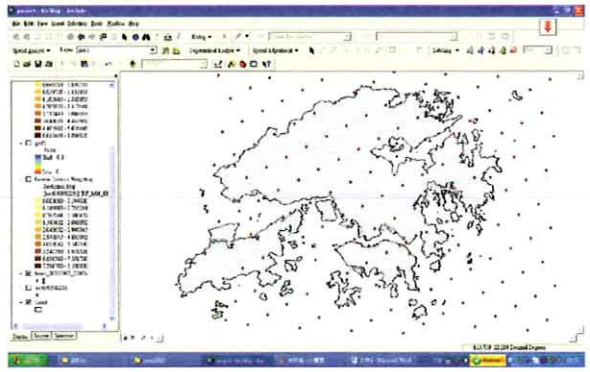

Figure 4. TRMM PR location converted to ArcView shapefile

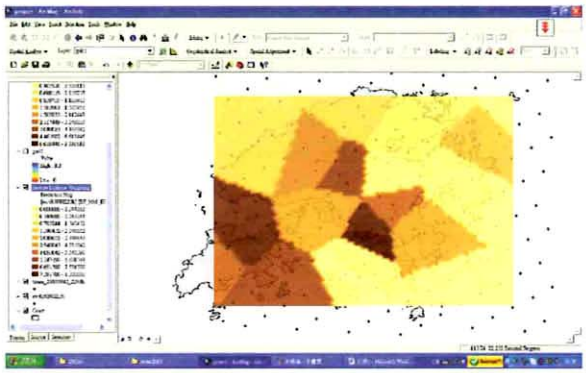

Figure 5. Inverse Distance Weighted Method (IDWM) with one neighbour for the AWS gauges

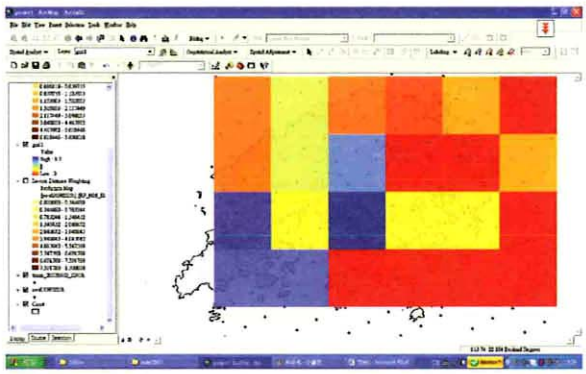

Figure 6. ArcView layer of 0.1 degree grid rainfall map derived from gauge data

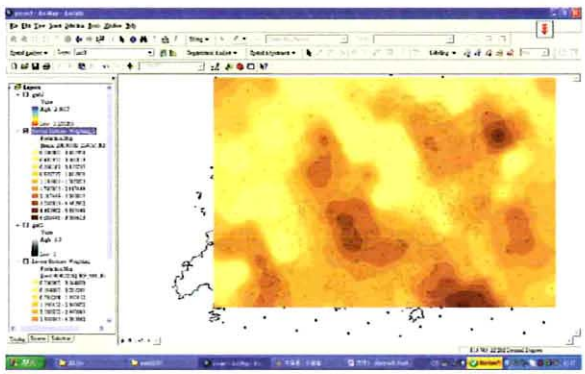

Figure 7. IDWM rainfall map of TRMM with 3 neighbors

map and binned into 0.1 degree maps in a similar fashion.

III. RESULTS

We first examined the geospatial statistics of gauge rain rates. Figure 8 shows the autocorrelation function as a function of separation for the gauge network for individual years (left panel) and for the whole ten years. The autocorrelation is defined as

$$\rho(\delta_{ij}) = \mathrm{cov}[(GD_i\ GD_j)]/\mathrm{var}(GD)$$

where GD_i is the rain rate at station i, cov is the covariance function at spatial separations of δ_{ij}, the distance between station i and j, $i \neq j$, and var is the variance of GD. The statistics are assumed isotropic and the ensembles, $[x]$ are averaged over time and all realization of separation distance (station pairs).

The e-folding distance, defined as the separation between gauges when the spatial autocorrelation falls below 1/e, is about 28 km, or roughly between 0.2 to 0.3 degree latitude. For separations much larger than the e-folding distance, the covariates are essentially decoupled. Hence comparison of hourly data for 0.1–0.4 degree grid data is appropriate.

To examine the spatial structure, we binned the data into 0.1, 0.2 and 0.4 degree boxes. A three-hourly 0.5 degree averaged gauge rain rate was also calculated for comparison with TMPA. The statistics used to compare different rainfall estimation

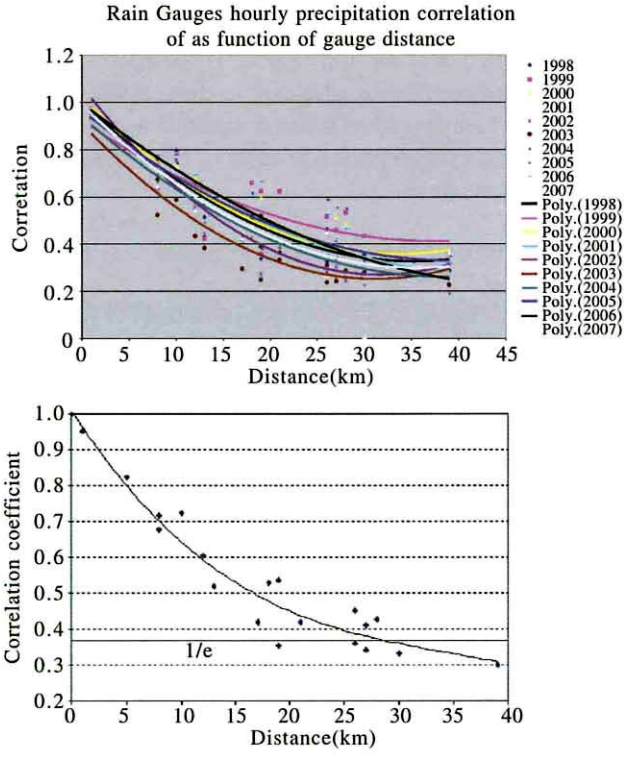

Figure 8. Spatial autocorrelation function of hourly rain gauges data as function of gauge separations. The left panel shows the autocorrelation for each year and the right panel show data averaged over all years. The curves show a best exponential fit to the data points

schemes include correlation coefficient (r^2), mean error (or bias), mean absolute difference (*MAE*), and root mean square difference (*RMSD*) defined below. While gauge data are also prone to error, they are used as the reference data here.

$$r^2 = \frac{\mathrm{cov}(SD_i, GD_i)}{\sigma_{SD}\sigma_{GD}}$$

$$Bias = \frac{1}{n}\sum_{i=1}^{n}(SD_i - GD_i)$$

$$MAE = \frac{1}{n}\sum_{i=1}^{n}|SD_i - GD_i|$$

$$RMSD = \sqrt{\frac{1}{n}\sum_{i=1}^{n}(SD_i - GD_i)^2}$$

Here n is the number of stations, SD is the satellite (TRMM) near surface rainfall data, and GD is the gauge rainfall data, σ_{SD} and σ_{GD} are their standard deviations and cov is the covariance function. The correlation coefficient has a value between −1 and 1 and indicates a positive or negative relation between two variables. The bias indicates the average direction of the deviation from observed values, but may not reflect the magnitude of the error. The mean absolute difference (*MAE*) measures the average magnitude of the difference in a set of estimated values, without considering their direction. The MAE is a linear score and all the individual differences are weight equally in the average. The root mean square difference (*RMSD*) is a quadratic scoring rule which measures the average magnitude of the error. Compare to the *MAE*, the *RMSD* gives greater weight to large differences than to small ones.

Table 2 shows the *Bias*, *RMSD* and *MAD* between PR and gauge data sets at 0.1, 0.2 and 0.4 degree grid bins. There is a general decrease of *RMSD* and *MAD* when the size of grid is increased. Overall, the biases are small, especially for TMPA. Figure 9 shows the annual correlation between gauge and TRMM 2A25 for 0.1, 0.2 and 0.4 degree grids and TMPA for 0.5 degree. The correlation coefficient increased when the grid size increased. The poor correlation in 2003 and 2004 may be due to poor sampling of rain events in these years.

Table 2. Summary statistics of biases, root mean square difference (*RMSD*) and mean absolute difference (*MAD*) between TRMM product and rain gauge analysis

2A25	*Bias*				*RMSD*				*MAD*			
	0.1°grid	0.2°grid	0.4°grid	3B42V6	0.1°grid	0.2°grid	0.4°grid	3B42V6	0.1°grid	0.2°grid	0.4°grid	3B42V6
1998	−0.2530	−0.2530	−0.2530	−0.0681	8.7698	4.3430	2.4968	1.1335	2.4111	1.7235	1.5089	0.2673
1999	−0.3406	−0.3406	−0.3406	−0.0464	3.5266	1.6482	0.9654	1.0301	1.7186	1.0497	0.6875	0.2229
2000	0.0509	0.0509	0.0509	−0.0670	2.9916	1.1043	0.5783	1.2037	1.1762	0.6144	0.4666	0.2632
2001	0.5751	0.5751	0.5751	−0.0617	5.6401	3.3270	2.1307	1.2970	2.0137	1.3701	1.0195	0.2695
2002	−0.1137	−0.1137	−0.1137	0.0015	4.5955	1.8143	0.7021	0.9637	2.0227	1.1051	0.3801	0.2293
2003	0.3562	0.3562	0.3562	−0.0059	4.9926	2.9842	2.3045	1.0997	2.2283	1.8097	1.5595	0.2015
2004	0.5189	0.5189	0.5189	0.0067	6.6968	4.8655	2.5642	0.7049	2.8623	2.4564	1.4528	0.1498
2005	−0.1604	−0.1604	−0.1604	0.1124	1.7662	1.2241	0.8722	0.8615	0.8677	0.7231	0.5704	0.2107
2006	0.1862	0.1862	0.1862	0.0731	2.3619	1.6123	1.0365	0.8237	0.9212	0.7334	0.5763	0.1950
2007	−0.1844	−0.1844	−0.1844	0.0503	2.5201	1.7560	1.1951	0.5634	0.9966	0.8536	0.7768	0.1361
mean	0.0635	0.0635	0.0635	−0.0005	4.3861	2.4679	1.4846	0.9681	1.7219	1.2439	0.8998	0.2145

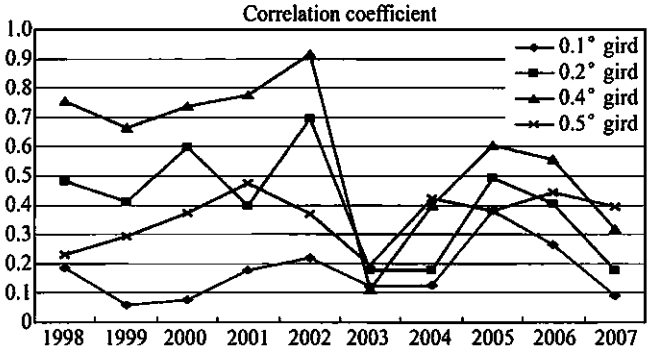

Figure 9. Annual correlation of 2A25 and 3B42 V6 with AWS rain gauges. The overall correlations are 0.16, 0.34, to 0.52 for 0.1, 0.2 and 0.4 degree boxes for PR and 0.35 for 0.5 degree boxes for TMPA

Bell and Kundu (2003) consider the sampling error when comparing monthly means from a satellite and a single gauge. For a satellite with once-daily overpasses, they estimate the relative sampling error to be on the order of 30% for averaging areas between about 200 and 500km in diameter. The error increases rapidly for smaller averaging areas (Bowman Kenneth P, 2005). As the averaging area increases, the size of the TRMM sample increases, reducing the sampling error. But as the area increases a single gauge becomes less representative of precipitation within the area, and the sampling error of the gauge increases (Bowman Kenneth P, 2005).

Figure 10 showed the scatterplots between TRMM PR and AWS for all ten years at 0.1, 0.2 and 0.4 degree resolutions. Correlation and linear regression analyses show correlation coefficients of 0.16, 0.34 and 0.52 and regression slopes of 0.32, 0.49 and 0.52 for 0.1, 0.2 and 0.4 degree grids, in that order.

Analysis of Rain Rate Probability Distribution Function (PDF) We examined the rain rate PDF of grid averages for 0.1, 0.2 and 0.4 degree grids and with TMPA at 0.5 degree. Figure 11 show the frequency distribution of rain intensity at

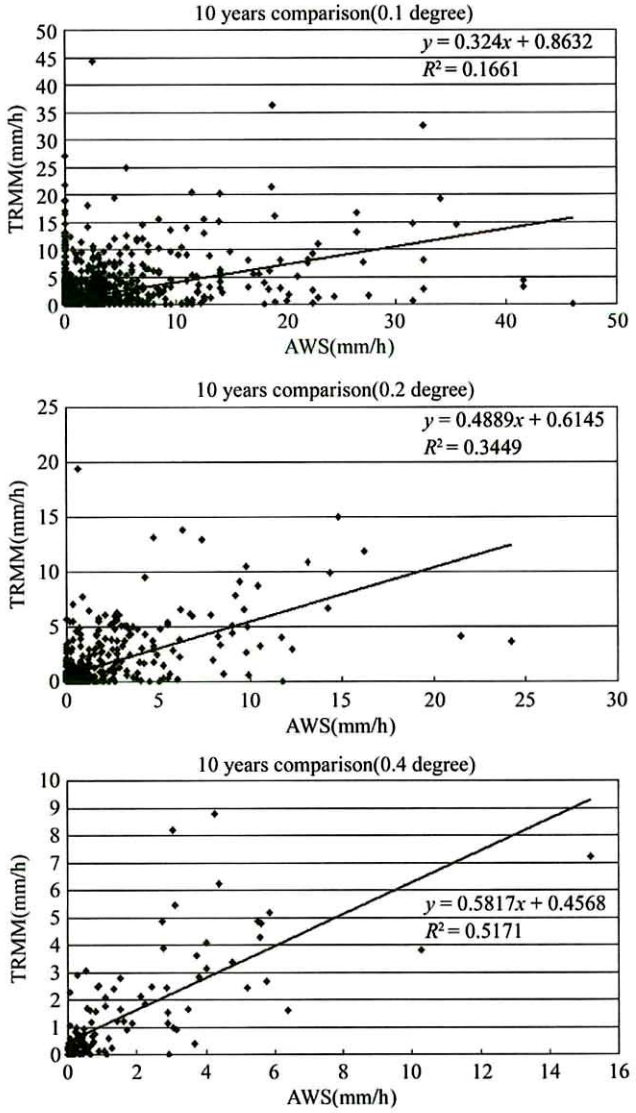

Figure 10. Scatterplots of PR and AWS gauge from 1998 to 2007 (10 years) at 0.1, 0.2 and 0.4 degree grids

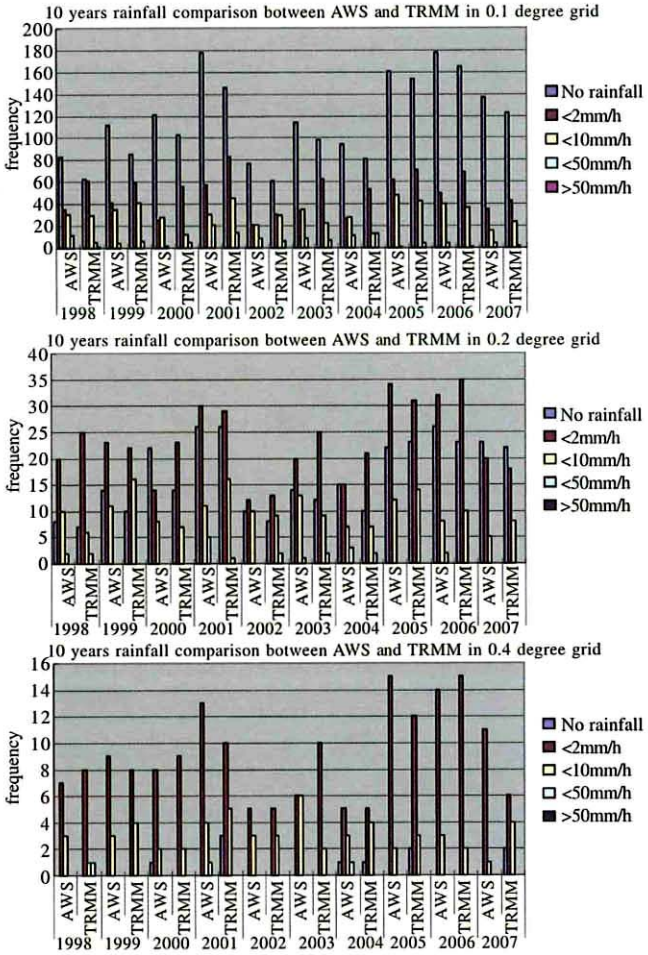

Figure 11. Frequency distribution of Rainfall Intensity in 0.1 degree (top panel), 0.2 degree (middle panel) and 0.4 degree (lower) grid. Blue bar represents gauge data, while brown bar represents the 2A25 data.
On the X-axis: "0" means no rainfall, "<2" means $0 < X < 2$ mm/h, "<10" means $2 \leqslant X < 10$ mm/h, "<50"means $10 \leqslant X < 50$ mm/h, ">50" means $X \geqslant 50$ mm/h

0.1, 0.2, 0.4 and 0.5 degree boxes. Rain rate are categorized into (i) light rain, with rain rate < 2.0 mm/h, (ii) moderate rain, with rate of fall between 2.0 and 10.0 mm/h, (iii) heavy rain, with rate of fall between 10.0 and 50.0 mm/h, and (iv) violent shower, when the rate >50.0 mm/h. For 0.1 degree grids, the numbers of zero rain occurrence recorded by the rain gauge are higher than the satellite estimates while the satellite sensors tend to show more observations at light and higher rain rates. As TRMM makes area averaged measurement, it tends to average localized high-precipitation regions with nearby regions having lower precipitation rates hence the no rain frequency is decreased. At 0.2 degree grid, the gauge data show higher frequency of no rain and light rain while the satellite data show higher frequency at the moderate and higher rain rate categories. At the 0.4 degree grid, the no rain category is further reduced, the frequency of light rain increases further.

Figure 12 shows the cumulative distribution of gauge rain rates, satellite rain rates at 0.1, 0.2 and 0.4 degree grids and TMPA 0.25 degree at 3 hourly. The gauge rain frequencies are higher than the PR estimates at the no rain, light and moderate rain. The cumulative distribution functions (CDFs) of 0.1 and 0.2 degree grid cross over that of 0.4 degree at rain rates slightly than 10 mm/h. The TMPA shows less rain fraction and the absence of violent storm compared to the AWS. This is consistent with the underestimation of TMPA for heavy rain in analysis in Thailand (Chokngamwong and Chiu, 2008).

IV. SUMMARY AND DISCUSSION

Analysis of hourly gauge data collected by about 20 AWSs over ten years(1998–2007) in Hong Kong show a spatial decorrelation distance of 28 km. Comparison of the hourly gauge and TRMM Precipitation Radar orbit (swath) data were carried out. Only coincident subset of PR swath with rain with

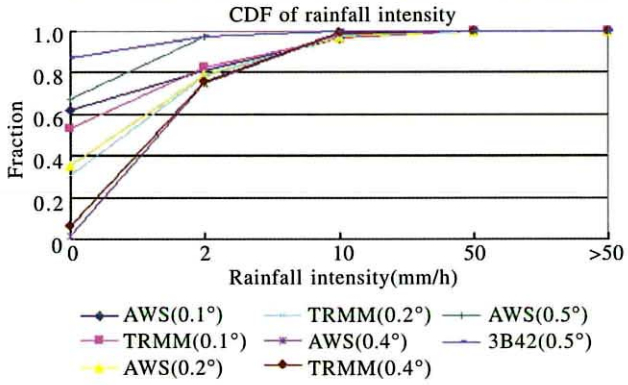

Figure 12. Cumulative Distribution Frequency of rainfall intensity for different grid sizes. The number in the blanket indicates the grid size

full coverage of the study area was considered. The data are interpolated using inverse distance methods and mapped onto 0.1, 0.2 and 0.4 degree grids and compared. The gauge data are also averaged to 0.5 degree grid 3 hourly data and compared with the TRMM Multi-satellite Precipitation Analysis (TMPA).

The International Precipitation Working Group (Ebert E, et al., 2007) compared near real-time rain estimates at the daily scale and found that satellite estimates tend to show better statistics over models in the rain season while model data are better in the dry season. Our results show that bias between TMPA and gauge is small (-0.005 mm h^{-1}) while PR tends to slightly overestimate the hourly gauge (0.06 mm h^{-1}). The correlation coefficient between PR estimates and hourly AWS gauge at 0.4 degree grid is about 0.5. This can be compared with a correlation coefficient of 0.35 for TMPA (3 hourly 0.25 degree). The IPWG comparison shows correlations of about 0.5 for daily 0.25 degree grids (Ebert E, et al., 2007, Figure 6). Both the RMSD and MAE decreased and the correlation coefficients increased as the grid size is increased. The correlation of 0.35 is consistent with other ground validation estimates.

This study is a preliminary comparison of gauge data with satellite swath data and 3 hourly merged satellite data analysis. It illustrates the potential of satellite rain observations for providing the rain rate characteristics for regional applications. The study only includes comparison when PR swath data provide full coverage of the study area and when both data show existence of rain. Both AWS and satellite data are mapped to a common earth grid (of 0.1, 0.2, and 0.4 degrees). Further studies need to include algorithm performance of rain event detection and sensitivity at other space and time scales. The comparison should also be performed with gauge data mapped to the satellite pixels.

ACKNOWLEDGMENTS

This work is part of an MPhil thesis submitted to GRM and ISEIS at CUHK. We thank Dr. R. Chokngamwong for helpful discussion and computing and graphics help. The data used in this study were acquired by the Tropical Rainfall Measuring Mission (TRMM). The data were processed by the TRMM Science Data and Information System (TSDIS) and archived and distributed by the Goddard Distributed Active Archive Center. TRMM is an international project jointly sponsored by the Japan Aerospace Exploration Agency (JAXA, previously known as National Space Development Agency or NASDA) and the U.S. National Aeronautics and Space Administration (NASA) Office of Earth Sciences. The images and data used in this study were processed using the GES-DISC Interactive Online Visualization ANd aNalysis Infrastructure (Giovanni) as part of the NASA's Goddard Earth Sciences (GES) Data and Information Services Center (DISC). TSDIS OrbitViewer is developed by TSDIS. LSC acknowledges support from the TRMM program.

REFERENCES

[1] Adler, Robert F., George J. Huffman, David T. Bolvin, Scott Curtis, Eric J. Nelkin, 2000, Tropical Rainfall Distributions Determined Using TRMM Combined with Other Satellite and Rain Gauge Information. Journal of Applied Meteorology, 39 (12): 2007–2023.

[2] Amitai, Eyal, 1999, Relationships between Radar Properties at High Elevations and Surface Rain Rate: Potential Use for Spaceborne Rainfall Measurements. Journal of Applied Meteorology, 38(3): 321–333.

[3] Bell, Kundu, 2003, Comparing satellite rainfall estimates with rain gauge data: Optimal strategies suggested by a spectral model. Journal of Geophysical Research, 108, 4121, doi: 10.1029/2002JD002641.

[4] Bowman, Kenneth P, 2005, Comparison of TRMM Precipitation Retrievals with Rain Gauge Data from Ocean Buoys. Journal of Climate, 18(1): 178–190.

[5] Chiu LS, Kedem B, 1990, Estimating the Exceedance Probability of Rain Rate by Logistic-Regression, Journal of Geophysical Research-Atmospheres, 95(D3): 2217–2227.

[6] Chiu LS, North GR, Short DA, Mcconnell A, 1990, Rain Estimation from Satellites-Effect of Finite-Field of View, Journal of Geophysical Research-Atmospheres, 95(D3): 2177–2185.

[7] Chiu, Long S., Alfred T. C. Chang, 2000, Oceanic Rain Column Height Derived from SSM/I. Journal of Climate, 13(23): 4125–4136.

[8] Chokngamwong R., Chiu L., 2008, Thailand Daily Rainfall and Comparison with TRMM Products, Journal of Hydrometeorology, 9, pp. 256–266.

[9] Ciach, Grzegorz J., Witold F. Krajewski, Emmanouil N. Anagnostou, Mary L. Baeck, James A. Smith, Jeffrey R. McCollum, Anton Kruger, 1997, Radar Rainfall Estimation for Ground Validation Studies of the Tropical Rainfall Measuring Mission. Journal of Applied Meteorology, 36(6): 735–747.

[10] Datta, Saswati, Jones, W. Linwood, Roy, Biswadev, Tokay, Ali, 2003, Spatial Variability of Surface Rainfall as Observed from TRMM Field Campaign Data. Journal of Applied Meteorology, 42(5): 598–610.

[11] David B. Wolff, D. A. Marks, E. Amitai, D. S. Silberstein, B. L. Fisher, A. Tokay, J. Wang and J. L. Pippitt. 2005: Ground Validation for the Tropical Rainfall Measuring Mission (TRMM). Journal of Atmospheric and Oceanic Technology,

22(4): 365–380.

[12] Ebert, E., J. Janowiak, C. Kidd, 2007, Comparison of near-real time precipitation estimates from satellite observations and models, Bulletin of the American Meteorological Society, 88, 48–64.

[13] Eyal Amitai, David A. Marks, David B. Wolff, David S. Silberstein, Brad L. Fisher, and Jason L. Pippitt, 2006, Evaluation of Radar Rainfall Products: Lessons Learned from the NASA TRMM Validation Program in Florida. Journal of Atmospheric and Oceanic Technology, 23(11): 1492–1505.

[14] Gebremichael, M., et al., 2008, Scaling of tropical rainfall as observed by TRMM precipitation radar, Atmospheric Research, doi:10.1016/j.atmosres. 2007.11.028.

[15] Hou, A. Y., S. Zhang, A. da Silva, W. Olson, C. Kummerow, J. Simpson, 2001, Improving global analysis and short-range forecast using rainfall and moisture observations derived from TRMM and SSM/I passive microwave sensors. Bull. Amer. Meteor. Soc., 82.

[16] Huffman G. J, Robert F. Adler, David T. Bolvin, Guojun Gu, Eric J. Nelkin, Kenneth P. Bowman, Yang Hong, Erich F. Stocker, David B. Wolff, 2007, The TRMM Multisatellite Precipitation Analysis (TMPA): Quasi-Global, Multiyear, Combined-Sensor Precipitation Estimates at Fine Scales. Journal of Hydrometeorology, 8(1): 38–55.

[17] Huffman, George J., Robert F. Adler, Bruno Rudolf, Udo Schneider, Peter R. Keehn, 1995, Global Precipitation Estimates Based on a Technique for Combining Satellite-Based Estimates, Rain Gauge Analysis, and NWP Model Precipitation Information. Journal of Climate, 8(5): 1284–1295.

[18] Iguchi, T., R. Meneghini, J. Awaka, T. Kozu, K. Okamoto, 2000, Rain profiling algorithm for TRMM precipitation radar data: Remote Sensing and Applications: Earth, Atmosphere and Oceans, 25, pp. 973–976.

[19] Ikai, Junji, Nakamura, Kenji. 2003, Comparison of Rain Rates over the Ocean Derived from TRMM Microwave Imager and Precipitation Radar. Journal of Atmospheric and Oceanic Technology, 20(12): 1709–1726.

[20] Kawanishi, T., H. Kuroiwa, M. Kojima, K. Oikawa, T. Kozu, H. Kumagai, K. Okamoto, M. Okumura, H. Nakatsuka, K. Nishikawa, 2000, TRMM precipitation radar. Remote Sensing and Applications: Earth, Atmosphere and Oceans, 25, pp. 969–972.

[21] Kummerow, C., J. Simpson, O. Thiele, W. Barnes, A. T. C. Chang, E. Stocker, R. F. Adler, A. Hou, R. Kakar, F. Wentz, P. Ashcroft, T. Kozu, Y. Hong, K. Okamoto, T. Iguchi, H. Kuroiwa, E. Im, Z. Haddad, G. Huffman, B. Ferrier, W. S. Olson, E. Zipser, E. A. Smith, T. T. Wilheit, G. North, T. Krishnamurti, K. Nakamura, 2000, The Status of the Tropical Rainfall Measuring Mission (TRMM) after Two Years in Orbit. Journal of Applied Meteorology, 39(12): 1965–1982.

[22] Kummerow, Christian, William Barnes, Toshiaki Kozu, James Shiue, Joanne Simpson, 1998, The Tropical Rainfall Measuring Mission (TRMM) Sensor Package. Journal of Atmospheric and Oceanic Technology, 15(3): 809–817.

[23] Masafumi Hirose, Kenji Nakamura, 2004, Spatiotemporal Variation of the Vertical Gradient of Rainfall Rate Observed by the TRMM Precipitation Radar. Journal of Climate, 17(17): 3378–3397.

[24] Mekonnen Gebremichael, Witold F. Krajewski, 2004, Assessment of the Statistical Characterization of Small-Scale Rainfall Variability from Radar: Analysis of TRMM Ground Validation Datasets. Journal of Applied Meteorology, 43(8): 1180–1199.

[25] Nystuen, Jeffrey A., John R. Proni, Peter G. Black, John C. Wilkerson, 1996, A Comparison of Automatic Rain Gauges. Journal of Atmospheric and Oceanic Technology, 13(1): 62–73.

[26] Robinson M., M.S. Kulie, D.S. Silberstein, D.A. Marks, D.B. Wolff, E. Amatai, B.S. Ferrier, B.L. Fisher, and J. Wang, 2000, Evolving improvements to TRMM ground validation of rainfall estimates. Physics and Chemistry of the Earth Part B-Hydrology Oceans and Atmosphere, 25, pp. 971–976.

[27] Schumacher, C., R. A. Houze, Jr., 2003, The TRMM Precipitation Radar's view of shallow isolated rain. Journal of Applied Meteorology, 42, pp. 1519–1524.

[28] Schumacher, Courtney, Robert A. Houze Jr., 2000, Comparison of Radar Data from the TRMM Satellite and Kwajalein Oceanic Validation Site. Journal of Applied Meteorology, 39(12): 2151–2164.

[29] Shin Dong-Bin, Chiu Long S., Kafatos Menas, 2001, Comparison of the Monthly Precipitation Derived from the TRMM Satellite,: Geophys. Res. Lett., 28(5): 795.

[30] Short, David A., Kenji Nakamura, 2000, TRMM Radar Observations of Shallow Precipitation over the Tropical Oceans. Journal of Climate, 13(23): 4107–4124.

[31] Simpson, J., C. Kummerow, W. K. Tao, R. F. Adler, 1996, On the Tropical Rainfall Measuring Mission(TRMM). Meteorology and Atmospheric Physics, 60, pp. 19–36.

[32] Simpson, Joanne, Robert F. Adler, Gerald R. North, 1988, A Proposed Tropical Rainfall Measuring Mission (TRMM) Satellite. Bulletin of the American Meteorological Society, 69 (3): 278.